

# Class-Conditional Domain Adaptation on Semantic Segmentation

Yue Wang<sup>1</sup>, Yuke Li<sup>2</sup>, James H. Elder<sup>2</sup>, Runmin Wu<sup>1</sup>, Huchuan Lu<sup>1</sup>

<sup>1</sup>Dalian University of Technology, China,

<sup>2</sup>York University, Canada

## Abstract

*Semantic segmentation is an important sub-task for many applications, but pixel-level ground truth labeling is costly and there is a tendency to overfit the training data, limiting generalization. Unsupervised domain adaptation can potentially address these problems, allowing systems trained on labelled datasets from one or more source domains (including less expensive synthetic domains) to be adapted to novel target domains. The conventional approach is to automatically align the representational distributions of source and target domains. One limitation of this approach is that it tends to disadvantage lower probability classes. We address this problem by introducing a Class-Conditional Domain Adaptation method (CCDA). It includes a class-conditional multi-scale discriminator and the class-conditional loss. This novel CCDA method encourages the network to shift the domain in a class-conditional manner, and it equalizes loss over classes. We evaluate our CCDA method on two transfer tasks and demonstrate performance comparable to state-of-the-art methods.*

## 1. Introduction

Semantic segmentation is an important visual scene understanding task with wide application, especially in autonomous and assisted vehicle systems. Recent deep network approaches (e.g., [18, 46, 2]) have achieved impressive results, but require large training datasets with precise pixel-level ground-truth annotation and do not generalize well over large domain shifts in viewpoint, lighting, etc. [41]

These issues can potentially be addressed by unsupervised domain adaptation methods that attempt to identify and correct for a shift in the appearance of the visual input from source to target domains. A successful domain adaptation method will not only improve generalization, but allow larger and more easily obtained synthetic ground truth to be

used for training, even if it does not perfectly represent the appearance of real scenes. The well-generalized model can be trained with synthetic image dataset which has access to ground-truth label, and real-world image dataset whose ground-truth label remains unknown, to avoid labor costing and high time-consuming annotation job. The synthetic image dataset with ground-truth label is named as source domain, while the real-world image dataset without ground-truth label is named as target domain.

A common approach to solve the "domain shift" problem for deep network systems is to modify the weights of the network to render representations produced by the network for target domain vectors more similar to representations produced for source domain vectors. By further minimizing the distance between distributions of certain representations from both domains, a well-generalized model can be obtained. Some papers have focused on representations in the prediction space [35, 38] while others have focused on representations in feature (latent) space [13, 5, 21]. Representational dissimilarity can be assessed using correlation distances [34] or maximum mean discrepancy [10]. However, more recent work has tended to focus on generative adversarial methods [11] for unsupervised domain adaptation. This adversarial principle becomes prominent since it achieves promising result for pixel-level prediction tasks [13, 12, 35, 38, 31, 22].

One limitation of prior work on unsupervised domain adaptation for semantic segmentation is that domain adaptation tends to be more effective for more frequent classes [13, 35]. An underlying tendency can be observed that representations on classes with higher frequency can be easily extracted and adapted, while certain classes with lower frequency are inclined to be failed. For driving datasets such as Cityscapes [6], adaptation works fairly well for dominant classes such as road, car, buildings, vegetation, and sky, but less well for infrequent classes such as sign or bicycle.

To address this issue, we propose a novel Class-Conditional Domain Adaptation method (CCDA). It consists of a class-conditional multi-scale discriminator, and a

class-conditional loss function for both segmentation and adaptation. The basic idea of our class-conditional multi-scale discriminator is to measure the alignment of feature-level representations at both fine and coarse spatial scales. The fine-scale branch is to evaluate the adaptation on pixel-level, while in particular, for each coarse-scale patch in the image, the loss is weighted equally over all classes occurring (or estimated to occur) within the patch, regardless of the number of pixels associated with each class. Our class-conditional multi-scale discriminator not only encourages the network to realign representations of pixels belonging to the same class in a consistent, class-conditional way, but also provides equal attention on each class occurred in one patch. Meanwhile, the design of the class-conditional loss function is also to assist the network to evaluate the performance of both segmentation and adaptation on each class fairly.

In summary, our proposed CCDA method makes three main contributions:

- We proposed a novel class-conditional multi-scale discriminator that allows class-conditional domain shift to be learned.
- By equalizing the class-conditional loss for both segmentation and adaptation, we further improve the performance for less frequent classes.
- We demonstrate that our method achieves comparable performance to state-of-the-art algorithms on two semantic segmentation domain adaptation scenarios.

## 2. Related Work

While there has been substantial progress on domain adaptation for image classification [37, 8, 19, 20, 15, 45, 40, 27, 9], pixel-level tasks are more challenging due to the more direct dependence on local appearance. Nevertheless, increasing activity in autonomous vehicle applications has driven interest in domain adaptation for pixel-level segmentation of road scenes [13, 43, 5, 38, 48, 14, 35, 25, 32, 44, 47, 4, 22].

The most popular current approach relies on adversarial learning, where a discriminator is employed to align source and target representations either at the prediction-level [35, 38] or the feature-level [13, 5, 21]. In [35], Tsai *et al.* first provide a prediction-level representation alignment with GAN network for domain adaptation on semantic segmentation. Vu *et al.* [38] then employ an entropy minimization technique during adversarial learning to improve domain adaptation at the prediction level and Luo *et al.* [21] use an information bottleneck approach to more fully remove task-independent information from feature representations. Co-training adaptation using multi-view learning has also been employed [31, 30, 22].

Approaches like pixel-level adaptation and self-training provide different directions for the process of domain adaptation, and can be combined with the above representation adaptation methods. The pixel-level adaptation approach is to view domain adaptation in part as a style transfer problem. In this approach, images from one domain are transformed to have the ‘style’ or appearance of images from another domain, while preserving the original ‘content’ of the image from the first domain [44, 32, 17]. The self-training approach is to alternatively select unlabelled target samples with higher prediction probability and utilize them with their predictions as pseudo ground-truth labels during training while updating the learnt model [48, 3].

Techniques like [5, 22, 7, 36] tend to boost domain adaptation performance for some classes or regions of the image more than others, suggesting that a class- or region-conditioned domain adaptation approach may be required to achieve good adaptation over all classes. In [5, 7], an adversarial system is employed to train distinct domain classifiers for each segmentation class. Luo *et al.* [22] instead use the disagreement between two classifiers to indicate the probability of incorrect representational alignment for each region of the image, increasing the weight of the adversarial loss for regions that appear to be poorly aligned. Tsai *et al.* [36] utilize the multiple modes of patch-level prediction with a more accurate classification for the category distribution, and apply the adaptation based on the representation of this patch classification. Meanwhile, for the self-training method, Zou *et al.* [48] employ class-normalized confidence scores for pseudo ground-truth label selection to prevent the imbalanced selection of target domain samples on each class, which improves the performance on less frequent classes.

The common drawback of the pervious adversarial learning adaptation methods is they neglect the imbalance frequency of different classes even though they consider the class information. They fail to apply the equal attention on each class by not taking the class-based performance into account. Here we propose a class-conditional multi-scale discriminator and a class-conditional loss function for both segmentation and adaptation. By using the designed class label for each patch, we allow the discriminator to consider class-conditional information for adaptation equal to all classes. The way of equalizing the loss over classes also improves the performance for lower frequent classes. Our method is more efficient than [5, 7] since we avoid training multi domain classifiers for each class, and the multi-scale discriminator encourages to capture the domain shift and evaluate the adaptation in pixel-level as well as patch-level.

## 3. Methods

In this section, we present our proposed CCDA approach using class-conditional multi-scale discriminator and our

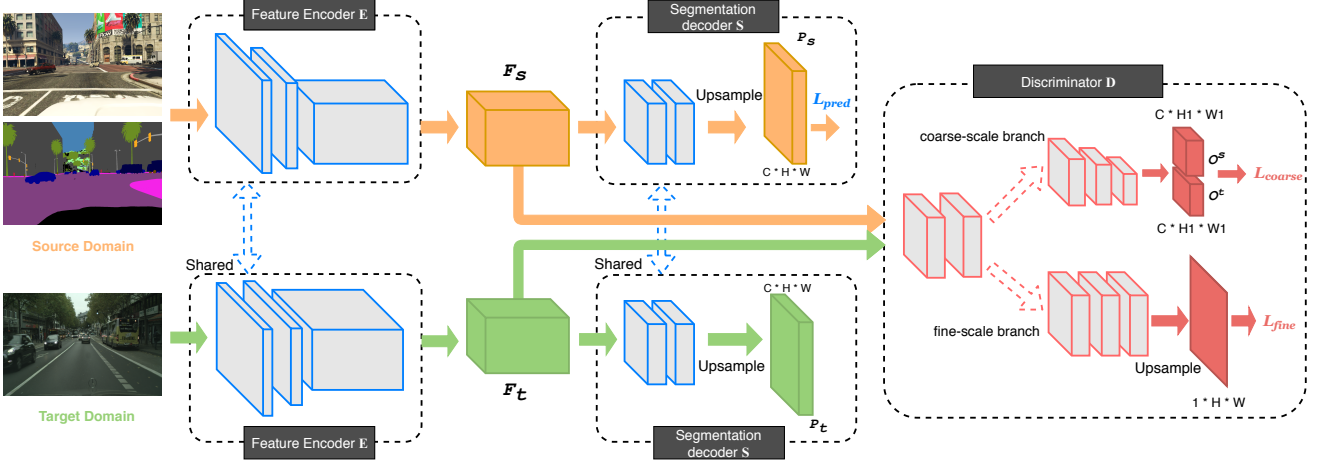


Figure 1. Overview of our proposed Class-Conditional Domain Adaptation.

class-conditional loss function for segmentation and adaptation. We begin by describing a basic structure for domain adaptation. Then, we will explain in detail innovations for our class-conditional multi-scale discriminator, and describe the design of class-based loss function for adaptation and segmentation components. The overview of our proposed structure is showed in Figure 1.

### 3.1. Basic Domain Adaptation Architecture

We apply an adversarial learning approach for our unsupervised domain adaptation on segmentation, since it is the most explored way in this area. A basic structure consists of three modules: a feature encoder  $\mathbf{E}$ , a segmentation decoder  $\mathbf{S}$ , and a discriminator  $\mathbf{D}$ . The image data consist of source domain data and target domain data. Each source image  $I_s \in \mathcal{I}_s$  is paired with ground truth pixel-level segmentation labels  $Y_s \in \mathcal{Y}_s$ . Target images  $I_t \in \mathcal{I}_t$  are assumed to have no ground truth data available for training.

Our goal is to train the feature encoder  $\mathbf{E}$  and segmentation decoder  $\mathbf{S}$  to output good prediction  $P_t$  on target domain image. This is achieved through two processes, one that trains  $\mathbf{E}$  and  $\mathbf{S}$  to output good segmentation prediction  $P_s$  for source image  $I_s$  with associated label  $Y_s$ , and a second that uses the discriminator  $\mathbf{D}$  to align the feature-level representations  $F_s$  and  $F_t$  output by the feature encoder  $\mathbf{E}$  for the two domains.

The first (segmentation) process is trained by minimizing the segmentation cross-entropy loss:

$$\mathcal{L}_{seg}(\mathbf{E}, \mathbf{S}) = - \sum_{h=1, w=1}^{H, W} \sum_{c=1}^C Y_s^{(h, w, c)} \log(P_s^{(h, w, c)}) \quad (1)$$

where  $H, W$  are the size of image,  $C$  is the number of semantic class.  $Y_s^{(h, w, c)}$  and  $P_s^{(h, w, c)}$  are the ground truth and

predicted states for Class  $c$  at pixel  $(h, w)$ .  $P_s = \mathbf{S}(F_s) = \mathbf{S}(\mathbf{E}(I_s))$  is the output of segmentation decoder  $\mathbf{S}$ .

The second (alignment) process is trained adversarially to generate domain-invariant features. Our discriminator module  $\mathbf{D}$  tries to distinguish feature representations from source and target domains, minimizing

$$\mathcal{L}_{D1}(\mathbf{D}) = \lambda_s \mathcal{L}_{bce}(\mathbf{D}(F_s), 0) + \lambda_t \mathcal{L}_{bce}(\mathbf{D}(F_t), 1) \quad (2)$$

where  $\mathcal{L}_{bce}$  is the binary cross-entropy domain classification loss since the output channel of this basic discriminator  $\mathbf{D}$  is 1. And source and target domain samples are assigned labels of 0 and 1, respectively. Concurrently, the feature encoder  $\mathbf{E}$  tries to confuse  $\mathbf{D}$ , minimizing

$$\mathcal{L}_{adv1}(\mathbf{E}) = \lambda_s \mathcal{L}_{bce}(\mathbf{D}(F_s), 1) + \lambda_t \mathcal{L}_{bce}(\mathbf{D}(F_t), 0) \quad (3)$$

This adversarial learning process produces a rough alignment of features among all classes, but tends to work less well for lower frequency classes that do not contribute substantially to the cross-entropy loss. Also, since the feature map computed by our encoder is spatiotopic but reduced in resolution relative to the input, the alignment achieved by our adversarial process is at the specific intermediate scale of our feature map, which may not capture domain shift at smaller or larger scales. These observations motivate our class-based multi-scale discriminator and class-based loss function for segmentation and adaptation.

### 3.2. Class-Conditional Multi-scale Discriminator

Our proposed class-conditional multi-scale discriminator is composed of fine-scale and coarse-scale branches (Fig. 1). The fine-scale branch measures alignment at the pixel-level using the basic architecture with loss functions in Equations 2 and 3 and thus can capture spatially detailed domain shift phenomena. The coarse-scale branch measures class-conditional alignment at a scale that is coarser

than the feature scale with the equal class information. We first describe how to perform this class conditioning by explaining the coarse-scale class label, and then elaborate on our structure of the class-based coarse-scale discriminator branch as well as the class-based fine-scale branch.

### 3.2.1 Coarse-Scale Class Labels

We define a coarse-scale class label  $W \in \{0, 1\}^C$  that indicates the presence or absence of each class within a rectangular patch of the image. Note that a patch may contain multiple classes, this class label is not a one-hot label. For source images,  $W$  is computed by analyzing the pixel-level ground-truth labels  $Y_s$  within the image back-projection of a patch. If any pixel within the back-projected region of the image has class  $c$ , we set  $W^c = 1$ , otherwise we set  $W^c = 0$ .

For target domain images, we do not have ground-truth labels. Instead, we assign coarse-scale class labels based on the projected pixel-level predictions  $P_t^c$  of our segmentation module **S** for the patch. In particular, given a confidence threshold  $th_w$ , if  $P_t^c > th_w$  for any pixel within a patch, we set  $W^c = 1$ , otherwise we set  $W^c = 0$ .

Note that binarizing the patch-based class label  $W$  has the effect of equalizing class frequencies at the patch level:  $W^c = 1$  whether the number of pixels with class  $c$  the patch contains. This will have the benefit or boosting adaptation performance for less frequent classes by apply an equal attention on all the classes a patch contains.

### 3.2.2 Class-conditional Coarse-scale Branch

For the basic domain adaptation in Section 3.1, the discriminator output is a scalar value indicating the domain of the input vector (in our case, 0 for source domain, 1 for target domain). In contrast, the output of our class-conditional coarse-scale discriminator branch consists of two vectors  $O^s$  and  $O^t$ , each of length  $C$ .  $O^s$  carries estimates of patch-level class labels for the source domain, an large value on  $O_c^s$  indicates high confidence that the patch contains at least one pixel drawn from the source domain and belonging to class  $c$ . And similarly,  $O^t$  carries estimates of patch-level class labels for the target domain.

The advantage of this dual vector representation is that it allows us to multiplex both domain and class information, informing both an adversarial adaptation loss based on class and a non-adversarial classification loss (Figure 2). In particular, to inform the non-adversarial classification loss, we form the vector  $O^c = \sigma(O^s + O^t)$ , where  $\sigma(\cdot)$  is a sigmoid function apply for each class. And we calculate a classification loss with the binary cross-entropy loss as  $\mathcal{L}_{bce}(O^c, W^c)$ . Note that including this classification loss in the discriminator will encourage a feature-level

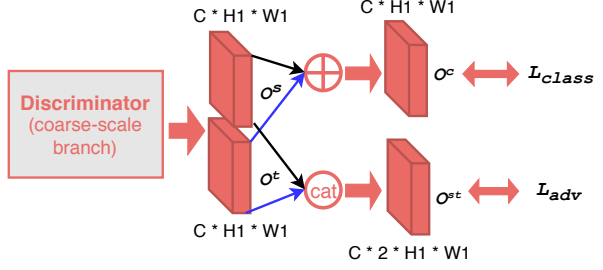


Figure 2. Details about the loss calculation in coarse-scale class-based branch in discriminator.

domain alignment that preserves segmentation class information. Meanwhile, the designed class label  $W$  insures the class information it preserves is equal to all classes, and improve the performance on less frequent classes.

To inform the adversarial adaptation loss, we form the  $C \times 2$  matrix  $O^{st} = f([O^s, O^t])$ , where  $f(\cdot)$  is the softmax operation over rows, normalizing the sum of  $O_c^s$  and  $O_c^t$  to 1 for every class  $c$ .  $O^{st}$  indicates the probability of the pixels belong to certain classes on a patch are from source domain or target domain. This normalization will tend to spread the loss more uniformly across classes. However, it should be noted that one patch may only contain certain classes instead of all  $C$  classes, so not all values on  $C$  channels are valuable for calculating the loss function for domain label classification. To form the final discriminator domain adaptation loss, we sum the class-conditional loss over classes present in the patch by the classes one contains, weighting the sum by the ground truth patch-level class labels  $W_s$  for the source domain, and the predicted patch-level class predictions  $O_t$  for the target domain. Combining with the non-adversarial classification loss, the total patch-level discriminator loss is:

$$\begin{aligned} \mathcal{L}_{D\_coarse}(\mathbf{D}) = & \lambda_c \mathcal{L}_{bce}(O^c, W^c) \\ & + \lambda_s \sum_{c=1}^C W_s^c[c] \mathcal{L}_{ce}(O_s^{st}[c], 0) \\ & + \lambda_t \sum_{c=1}^C O_t^c[c] \mathcal{L}_{ce}(O_t^{st}[c], 1) \end{aligned} \quad (4)$$

where  $O_s^{st}$  is the output  $O_{st}$  for source domain images and  $O_t^{st}$  is the output  $O_{st}$  for source domain images.

The generative component of the adversarial loss is defined symmetrically:

$$\begin{aligned} \mathcal{L}_{adv\_coarse}(\mathbf{E}, \mathbf{S}) = & \lambda_c \mathcal{L}_{bce}(O^c, W^c) \\ & + \lambda_s \sum_{c=1}^C W_s^c[c] \mathcal{L}_{ce}(O_s^{st}[c], 1) \\ & + \lambda_t \sum_{c=1}^C O_t^c[c] \mathcal{L}_{ce}(O_t^{st}[c], 0) \end{aligned} \quad (5)$$

### 3.2.3 Fine-Scale Class-Conditional Discriminator

The coarse-scale class-conditional adaptation can capture larger-scale domain shift effects but may not capture shifts in finer detail. For that purpose, we employ a fine-scale class-conditional discriminator which can evaluate the adaptation on a pixel-level way. It remains the scale of feature representations in this fine-scale discriminator branch and upsamples the output to produce a fine-scale domain classification  $U_s$  and  $U_t$  that match the size of the original input. For this fine-scale discriminator branch, we also evaluate the performance of adaptation for each class by a class-conditional loss.

For source domain images, we employ the ground-truth class labels  $Y_s$  to calculate the loss for each class and average over classes to form a class-conditional binary cross entropy loss:

$$\mathcal{L}_{cbce\_s}(U_s, Y_s, l_d) = \frac{1}{C} \sum_{c=1}^C \left( \frac{\sum_{h,w} Y_s^{(h,w,c)} \mathcal{L}_{bce}(U_s^{(h,w)}, l_d)}{\sum_{h,w} Y_s^{(h,w,c)} + \epsilon} \right) \quad (6)$$

where the ground truth domain label  $l_d$  is set to  $l_d = 0$  when training the discriminator  $\mathbf{D}$ , and to  $l_d = 1$  when training the encoder  $\mathbf{E}$  and segmentation module  $\mathbf{S}$ , to confuse the discriminator. For target domain images, we do not have ground-truth class labels, and so we employ the pixel-level class predictions  $P_t$  instead to form a pseudo-label  $\hat{Y}_t$  by selecting the class with the highest prediction value:

$$\hat{Y}_t^{h,w,c} = \begin{cases} 1 & \text{if } c = \arg \max P_t^{h,w} \\ 0 & \text{otherwise} \end{cases} \quad (7)$$

The above pixel-level class predictions will not be confident since the segmentation network is highly rely on source domain images. It can be used as an indication that domain shift is interfering with classification. Therefore, it is necessary to focus more on the adaptation of these uncertain regions by giving them a large weight. We identify these ambiguous pixels by a label  $N_t$ :

$$N_t^{h,w} = \begin{cases} 1 & \text{if } \max_c P_t^{h,w,c} < th_n \\ 0 & \text{otherwise} \end{cases} \quad (8)$$

where  $th_n$  is a threshold constant for selecting the uncertain pixels. We then add an additional term to the fine-scale domain adaptation loss that will serve to upweight these regions during feature alignment. The final class-conditional binary cross entropy loss for target domain becomes:

$$\begin{aligned} \mathcal{L}_{cbce\_t}(U_t, \hat{Y}_t, l_d) = & \frac{1}{C} \sum_{c=1}^C \left( \frac{\sum_{h,w} \hat{Y}_t^{(h,w,c)} \mathcal{L}_{bce}(U_t^{(h,w)}, l_d)}{\sum_{h,w} \hat{Y}_t^{(h,w,c)} + \epsilon} \right) \\ & + \lambda_n \frac{\sum_{h,w} N_t^{(h,w)} \mathcal{L}_{bce}(U_t^{(h,w)}, l_d)}{\sum_{h,w} N_t^{(h,w)} + \epsilon} \end{aligned} \quad (9)$$

The fine-scale class-conditional adaptation discriminator loss over all images is then:

$$\begin{aligned} \mathcal{L}_{D2}(\mathbf{D}) = & \lambda_s \mathcal{L}_{cbce\_s}(U_s, Y_s, 0) \\ & + \lambda_t \mathcal{L}_{cbce\_t}(U_t, \hat{Y}_t, 1) \end{aligned} \quad (10)$$

The generative component of the adversarial fine-scale loss trained on feature encoder  $\mathbf{E}$  and segmentation decoder  $\mathbf{S}$  is defined symmetrically:

$$\begin{aligned} \mathcal{L}_{adv2}(\mathbf{E}, \mathbf{S}) = & \lambda_s \mathcal{L}_{cbce\_s}(U_s, Y_s, 1) \\ & + \lambda_t \mathcal{L}_{cbce\_t}(U_t, \hat{Y}_t, 0) \end{aligned} \quad (11)$$

For stability, we blend these class-conditional fine-scale losses with the conventional losses from the basic architecture defined in Equations 2 and 3:

$$\mathcal{L}_{D\_fine}(\mathbf{D}) = \beta \mathcal{L}_{D1} + (1 - \beta) \mathcal{L}_{D2} \quad (12)$$

$$\mathcal{L}_{adv\_fine}(\mathbf{E}, \mathbf{S}) = \beta \mathcal{L}_{adv1} + (1 - \beta) \mathcal{L}_{adv2} \quad (13)$$

By utilizing the class-conditional loss, we manage to evaluate the performance among all classes equally for our fine-scale discriminator branch to further improve the performance on less frequent classes.

### 3.3. Class-Conditional Segmentation Loss

The conventional loss employed for pixel-level semantic segmentation is the pixel-level cross-entropy loss. The final value of segmentation loss will be the mean loss of all pixels regardless of the class information. Unfortunately, this has the drawback that classes that are less frequent at the pixel-level, either because regions of that class occur infrequently or because they tend to be small, do not contribute substantially to the loss function, while the pixels belongs to classes which are high frequent dominate the training process. And thus performance of the trained system for the less frequent classes can be poor, since the pixels belongs to less frequent classes tend to be neglect during the training process. For domain adaptation systems, this has the additional consequence that the system may never learn how to align representations across domains for these infrequent classes.

To begin to address this problem, we introduce a modified class-conditional loss for segmentation, which will serve to distribute the loss more evenly across classes. In particular, we employ a blend of the dice loss [24] and the cross-entropy loss to train our segmentation network. The idea of dice loss comes from the dice coefficients, and has been widely used in medical image segmentation [26, 39]. It has the form:

$$\mathcal{L}_{dice}(\mathbf{E}, \mathbf{S}) = 1 - \frac{1}{C} \sum_{c=1}^C \left( \frac{2 \sum_{h,w} Y_s^{(h,w,c)} P_s^{(h,w,c)}}{\sum_{h,w} (Y_s^{(h,w,c)} + P_s^{(h,w,c)}) + \epsilon} \right) \quad (14)$$

Note that the loss is formed as the complement of a normalized segmentation performance averaged over classes. The normalization, similar in spirit to intersection-over-union, will roughly equalize the contribution of each class to the loss function.  $\epsilon$  is a small constant that prevents division by 0 for classes that do not appear in ground truth or predictions within an image.

Since the up-weighting of rare classes may introduce instability in training, we elect to employ a blend of the dice loss with the conventional cross-entropy loss (Equation (1)) to form the segmentation prediction loss  $\mathcal{L}_{pred}$ :

$$\mathcal{L}_{pred}(\mathbf{E}, \mathbf{S}) = \alpha \mathcal{L}_{seg} + (1 - \alpha) \mathcal{L}_{dice} \quad (15)$$

By this class-conditional loss for segmentation, we manage to evaluate the performance of prediction among all classes equally on source domain images, which further improve the performance of segmentation prediction for target domain images after the adaptation.

### 3.4. Complete Training Loss

To summarize, the complete training process combines the class-conditional segmentation loss (Equation 15), fine- and coarse-scale class-conditional domain adaptation discriminator losses (Equations 12 and 4) and fine- and coarse-scale domain adaptation adversarial losses (Equation 13 and 5):

$$\min_{\mathbf{D}} \mathcal{L}_{D\_fine} + \mathcal{L}_{D\_coarse} \quad (16)$$

$$\min_{\mathbf{E}, \mathbf{S}} \mathcal{L}_{pred} + \mathcal{L}_{adv\_fine} + \mathcal{L}_{adv\_coarse} \quad (17)$$

## 4. Experiments

In this section, we evaluate our class-conditional domain adaptation method and present the experimental results. First, we introduce the used datasets and some implementation details of our network architecture. Then, we show the comparison with the state-of-art method and discuss the effectiveness for our CCDA method with the ablation study.

### 4.1. Datasets

Manual generation of pixel-level ground truth for semantic segmentation is expensive. Since for synthetic datasets, pixel-level labels can be derived directly from the generative model, synthetic data has the potential to vastly expand the quantity of labeled data used to train deep semantic segmentation networks. But translating this into greater accuracy at inference time requires bridging any domain shift between the synthetic training data and the real test data.

With this motivation, we evaluate our class-conditional domain adaptation method by employing two synthetic source domain datasets (SYNTHIA [29] and GTA5 [28])

and a real-world target domain dataset (Cityscapes [6]). This defines two adaptation tasks: GTA5  $\rightarrow$  Cityscapes, and SYNTHIA  $\rightarrow$  Cityscapes.

The GTA5 dataset is a large synthetic dataset with 24,966 images with pixel-level ground-truth labels. The image resolution is  $1914 \times 1052$  pixels and the class labels are compatible with the Cityscapes dataset. The SYNTHIA dataset is also a widely used synthetic dataset for domain adaptation, which contains 9,400 images with pixel-level ground-truth labels. The image resolution is  $960 \times 720$  pixels. For the real-world images, Cityscapes dataset comprises 2,975 training images and 500 validation images with the resolution of  $2048 \times 1024$  pixels.

To train our domain adaptation model, we employ both the images and the ground truth labels from either the GTA5 dataset or SYNTHIA datasets for the source domain, and only the images (not the labels) from the Cityscapes training set for the target domain. We evaluate our model on the Cityscapes validation set, over 19 classes for GTA5  $\rightarrow$  Cityscapes adaptation and over 13 and 16 classes for SYNTHIA  $\rightarrow$  Cityscapes, as per convention like in [35, 42].

### 4.2. Implementation Details

We apply PyTorch for our implementation using a single GeForce RTX 2080 Ti GPU with 11 GB memory. For segmentation, we use the DeepLab-v2 [2] framework with a small VGG16 [33] pre-trained model as backbone for our feature encoder  $\mathbf{E}$  and segmentation decoder  $\mathbf{S}$ . For discriminator module  $\mathbf{D}$ , the fine-scale branch has a structure similar to [35, 22], consisting of 5 convolution layers with channel numbers  $\{64, 128, 256, 512, 1\}$ . To preserve fine-scale detail, we use  $3 \times 3$  kernels and a stride of 1. A final up-sampling layer is added at the end of this branch to rescale the output to the input image resolution. For the coarse-scale branch, we share the first two convolution layers with the fine-scale branch, and then apply 3 convolution layers with channel numbers  $\{256, 512, C \times 2\}$  with kernel 3 and stride of 2 for downsampling. Except for the last convolution layer in both branches, each convolution layer in our discriminator module is followed by a Leaky-ReLU [23] with a slope of 0.2 for negative inputs.

To train our feature encoder  $\mathbf{E}$  and segmentation decoder  $\mathbf{S}$ , we use the Stochastic Gradient Descent (SGD) optimizer [1] with the momentum of 0.9 and the weight decay is  $5e-4$ . The initial learning rate is set to  $2.5e-4$  and decays during training. For discriminator module  $\mathbf{D}$ , we apply ADAM [16] optimizer with  $\beta_1 = 0.9$  and  $\beta_2 = 0.99$ . The initial learning rate is set to  $1e-4$  and decayed with the same policy as SGD. We train our model with a crop of  $512 \times 1024$  with one source domain image and one target domain image at a time the same as in [22, 21]. We set hyper-parameters  $\lambda_s = \lambda_t = 0.0003$  for both fine-scale and coarse-scale branch.

Table 1. Adaptation from GTA5 to Cityscapes. We present the per-class IoU and mean IoU. The numbers above all classes are the indexes of their frequency in a descending order based on Cityscapes. (Please refer to [6] for more details) "CT", "ST" and "AT" represent curriculum-learning method, self-training, and adversarial-learning method. "P" and "F" represent prediction-level adaptation and feature-level adaptation. We highlight the best result in each column in **bold**.

		GTA5 → Cityscapes																			
	Meth.	1 road	5 side.	2 buil.	11 wall	10 fence	7 pole	17 light	12 sign	3 vege.	9 terr.	6 sky	8 pers.	18 rider	4 car	15 truck	14 bus	16 train	19 mbike.	13 bike	mIoU
CDA [42]	CT	72.9	30.0	74.9	12.1	13.2	15.3	16.8	14.1	79.3	14.5	<b>75.5</b>	35.7	10.0	62.1	20.6	19.0	0.0	<b>19.3</b>	12.0	31.4
CBST-SP [48]	ST	<b>90.4</b>	50.8	72.0	18.3	9.5	<b>27.2</b>	<b>28.6</b>	14.1	<b>82.4</b>	25.1	70.8	42.6	<b>14.5</b>	76.9	5.9	12.5	<b>1.2</b>	14.0	<b>28.6</b>	36.1
Ours		90.0	<b>36.2</b>	<b>79.1</b>	<b>25.0</b>	<b>18.9</b>	26.8	27.6	<b>16.5</b>	80.8	<b>31.1</b>	73.4	<b>48.4</b>	12.8	<b>81.2</b>	<b>25.6</b>	<b>24.8</b>	0.0	12.5	5.4	<b>37.7</b>
AdaptSeg [35]	AT-P	87.3	29.8	78.6	21.1	18.2	22.5	21.5	11.0	79.7	29.6	71.3	46.8	6.5	80.1	23.0	26.9	0.0	10.6	0.3	35.0
ADVENT [38]		86.9	28.7	78.7	<b>28.5</b>	<b>25.2</b>	17.1	20.3	10.9	80.0	26.4	70.2	47.1	8.4	<b>81.5</b>	26.0	17.2	<b>18.9</b>	11.7	1.6	36.1
CLAN [22]		88.0	30.6	<b>79.2</b>	23.4	20.5	26.1	23.0	14.8	<b>81.6</b>	<b>34.5</b>	72.0	45.8	7.9	80.5	<b>26.6</b>	<b>29.9</b>	0.0	10.7	0.0	36.6
FCNs in the Wild [13]	AT-F	70.4	32.4	62.1	14.9	5.4	10.9	14.2	2.7	79.2	21.3	64.6	44.1	4.2	70.4	8.0	7.3	0.0	3.5	0.0	27.1
SIBIN [21]		83.4	13.0	77.8	20.4	17.5	24.6	22.8	9.6	81.3	29.6	<b>77.3</b>	42.7	10.9	76.0	22.8	17.9	5.7	<b>14.2</b>	2.0	34.2
Ours		<b>90.0</b>	<b>36.2</b>	79.1	25.0	18.9	<b>26.8</b>	<b>27.6</b>	<b>16.5</b>	80.8	31.1	73.4	<b>48.4</b>	<b>12.8</b>	81.2	25.6	24.8	0.0	12.5	<b>5.4</b>	<b>37.7</b>

Table 2. Adaptation from SYNTHIA to Cityscapes. The table setting is the same as Table 1, while mIoU and mIoU\* are averaged over 16 and 13 categories, respectively.

		SYNTHIA → Cityscapes																		
	Meth.	1	5	2	10	9	7	14	11	3	6	8	15	4	13	16	12			
		road	side.	buil.	wall*	fence*	pole*	light	sign	vege.	sky	pers.	rider	car	bus	mbike.	bike	mIoU	mIoU*	
CDA [42]	CT	57.4	23.1	74.7	0.5	<b>0.6</b>	14.0	5.3	4.3	77.8	73.7	45.0	11.0	44.8	<b>21.2</b>	1.9	20.3	29.7	35.4	
CBST-SP [48]	ST	69.6	28.7	69.5	<b>12.1</b>	0.1	<b>25.4</b>	<b>11.9</b>	<b>13.6</b>	<b>82.0</b>	<b>81.9</b>	<b>49.1</b>	<b>14.5</b>	66.0	6.6	3.7	<b>32.4</b>	<b>35.4</b>	36.1	
Ours		<b>82.6</b>	<b>34.2</b>	<b>76.9</b>	2.6	0.2	23.8	3.5	7.7	77.9	79.5	44.2	8.2	<b>73.4</b>	20.9	<b>4.0</b>	14.2	34.6	<b>40.6</b>	
AdaptSeg [35]	AT-P	78.9	29.2	75.5	-	-	-	0.1	4.8	72.6	76.7	43.4	8.8	71.1	16.0	3.6	8.4	-	37.6	
ADVENT [38]		67.9	29.4	71.9	<b>6.3</b>	<b>0.3</b>	19.9	0.6	2.6	74.9	74.9	35.4	<b>9.6</b>	67.8	<b>21.4</b>	<b>4.1</b>	<b>15.5</b>	31.4	36.6	
CLAN [22]		80.4	30.7	74.7	-	-	-	1.4	8.0	77.1	79.0	46.5	8.9	<b>73.8</b>	18.2	2.2	9.9	-	39.3	
FCNs in the Wild [13]	AT-F	11.5	19.6	30.8	4.4	0.0	20.3	0.1	<b>11.7</b>	42.3	68.7	<b>51.2</b>	3.8	54.0	3.2	0.2	0.6	20.2	22.9	
Cross-city [5]		62.7	25.6	78.3	-	-	-	1.2	5.4	<b>81.3</b>	<b>81.0</b>	37.4	6.4	63.5	16.1	1.2	4.6	-	35.7	
SIBIN [21]		70.1	25.7	<b>80.9</b>	-	-	-	<b>3.8</b>	7.2	72.3	80.5	43.3	5.0	73.3	16.0	1.7	3.6	-	37.2	
Ours		<b>82.6</b>	<b>34.2</b>	76.9	2.6	0.2	<b>23.8</b>	3.5	7.7	77.9	79.5	44.2	8.2	73.4	20.9	4.0	14.2	<b>34.6</b>	<b>40.6</b>	

### 4.3. Results

Table 1 and Table 2 summarizes the performance of our method compared with the state-of-the-art on the two transfer tasks GTA5 → Cityscapes, and SYNTHIA → Cityscapes, respectively. For a fair comparison, we choose several state-of-art methods using the same VGG16 as backbone as our method, which include adversarial-learning methods with prediction-level adaptation AdaptSeg [35], ADVENT [38], CLAN [22]; and adversarial-learning methods with feature-level adaptation FCNs in the Wild [13], Cross-city [5], SIBIN [21]. We do not compare with the two latest state-of-art method [7, 36], since they use

different setting of Cityscape dataset or add extra pixel-level adaptation (image style-transfer) module. We also compare our method with self-training method CBST-SP [48]; curriculum-learning method CDA [42]. These two methods achieve better performance on lower frequency classes due to their strategy of alternate selection of target domain samples for training the segmentation.

In Table 1, we present our experimental results on the GTA5 → Cityscapes task compared with the chosen state-of-art methods. This table shows our proposed CCDA method performs better on average than all of these methods, and this advantage derives from improvements over a wide range of classes. We observe that our class-conditional method boosts the performance of lower-frequency classes substantially while maintaining performance for higher-frequency classes like road, building, vegetation, car, and thus ultimately a higher mean IoU performance.

In Table 2, comparison with current state-of-the-art methods on SYNTHIA → Cityscapes transfer task shows that our CCDA method performs favorably against the other algorithms on mIoU, which indicates that our method increases the overall performance. Especially, compared with

Table 3. Ablation Study on our CCDA method.

Task	Method			mIoU
	$\mathcal{L}_{basic}$	$\mathcal{L}_{basic\_class}$	$\mathcal{L}_{coarse}$	
GTA5 → Cityscapes	✓			34.9
	✓	✓		37.0
	✓	✓	✓	37.7



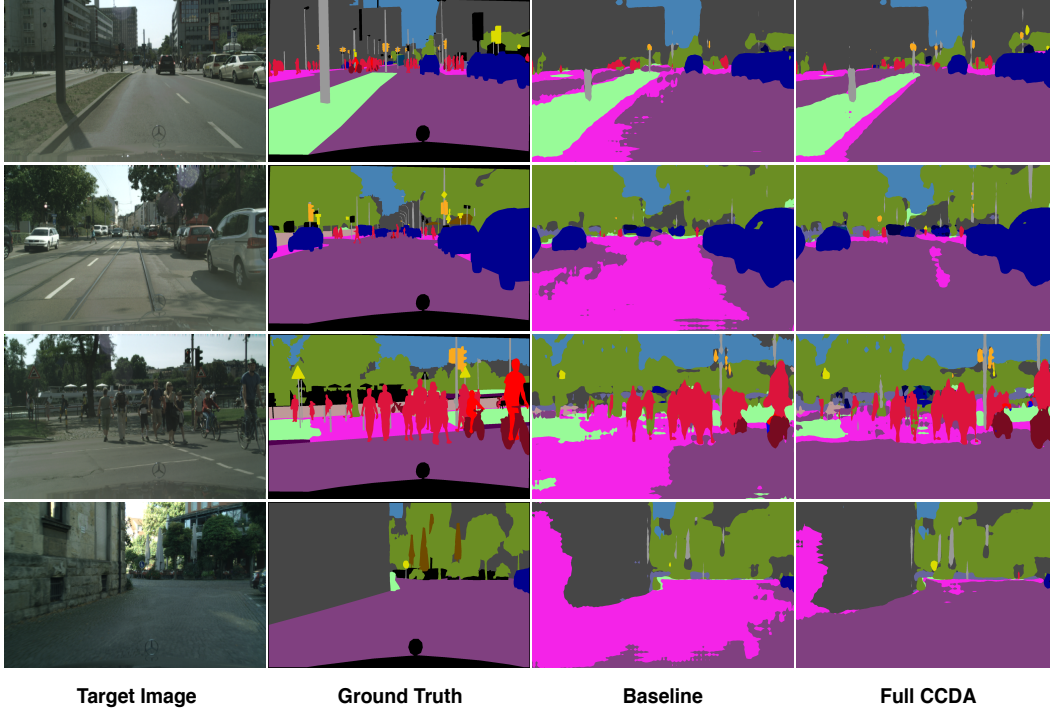


Figure 3. Example results of our proposed Class-Conditional Domain Adaptation (CCDA). for GTA5  $\rightarrow$  Cityscapes task. For each target image, we show the corresponding Ground-truth map, the result for the baseline CCDA architecture in Section 3.1, and the result for our full CCDA system.

other adversarial learning methods, our CCDA has advantages on lower-frequency classes. While for self-training and curriculum-learning method which perform better on several least frequent classes, we can still reach a comparable results on these classes and outperform them on the overall performance.

#### 4.4. Ablation Studies

To better understand the impact of each component of our adaptation model, we conducted an ablation study by selectively deactivating each component and measuring the effect on performance for the GTA5  $\rightarrow$  Cityscapes transfer task. In particular, we define three nested subset models:

1)  $\mathcal{L}_{basic}$ : using the basic domain adaptation architecture in Section 3.1 with the segmentation loss and a fine-scale basic discriminator.

2)  $\mathcal{L}_{basic} + \mathcal{L}_{basic\_class}$ : adding class-conditional loss for segmentation in Section 3.3 as well as the class-conditional loss for fine-scale discriminator in Section 3.2.3 on the basic architecture.

3)  $\mathcal{L}_{basic} + \mathcal{L}_{class\_based} + \mathcal{L}_{coarse}$ : further adding the class-conditional coarse-scale branch for discriminator in Section 3.2.2.

The result is showed in Table 3. Our class-conditional loss on the basic architecture (both segmentation and fine-scale discriminator) gains 2.1% improvements together and

the designed coarse-scale branch brings another 0.7% improvements. It verifies the effectiveness of our CCDA method, including both class-based loss and the class-based coarse-scale branch. We also present some qualitative segmentation examples in Figure 3. This figure also verifies the effectiveness of our CCDA method. The performance of our CCDA method outperforms the baseline structure in two ways. Firstly, it provides a cleaner and more accurate prediction on higher-frequency like road and sidewalk. Secondly, it improves the performance of lower-frequency classes like light and sign.

## 5. Conclusions

We have developed a novel approach to solving an important problem in domain adaptation for semantic segmentation, namely, the poor performance often observed for infrequent classes. The solution hinges on the introduction of class-conditioning at multiple points in the model, including segmentation, coarse-scale domain adaptation and fine-scale domain adaptation, and upon equalizing across classes at several stages in the computation. Evaluation on two transfer tasks demonstrates the effectiveness of our method, which boosts performance on infrequent classes while maintaining performance on the remaining classes. Generally, the proposed class-conditional domain adapta-



tion method outperforms the state of the art on average, due to superior performance on a broad range of classes.

**Acknowledgements:** We would like to thank the York University Vision: Science to Applications (VISTA) program for its support.

## References

- [1] Léon Bottou. Large-scale machine learning with stochastic gradient descent. In *Proceedings of COMPSTAT'2010*, pages 177–186. Springer, 2010.
- [2] Liang-Chieh Chen, George Papandreou, Iasonas Kokkinos, Kevin Murphy, and Alan L Yuille. Deeplab: Semantic image segmentation with deep convolutional nets, atrous convolution, and fully connected crfs. *IEEE transactions on pattern analysis and machine intelligence*, 40(4):834–848, 2018.
- [3] Minghao Chen, Hongyang Xue, and Deng Cai. Domain adaptation for semantic segmentation with maximum squares loss. *arXiv preprint arXiv:1909.13589*, 2019.
- [4] Yuhua Chen, Wen Li, and Luc Van Gool. Road: Reality oriented adaptation for semantic segmentation of urban scenes. In *Proceedings of the IEEE Conference on Computer Vision and Pattern Recognition*, pages 7892–7901, 2018.
- [5] Yi-Hsin Chen, Wei-Yu Chen, Yu-Ting Chen, Bo-Cheng Tsai, Yu-Chiang Frank Wang, and Min Sun. No more discrimination: Cross city adaptation of road scene segmenters. In *Proceedings of the IEEE International Conference on Computer Vision*, pages 1992–2001, 2017.
- [6] Marius Cordts, Mohamed Omran, Sebastian Ramos, Timo Rehfeld, Markus Enzweiler, Rodrigo Benenson, Uwe Franke, Stefan Roth, and Bernt Schiele. The cityscapes dataset for semantic urban scene understanding. In *Proceedings of the IEEE conference on computer vision and pattern recognition*, pages 3213–3223, 2016.
- [7] Liang Du, Jingang Tan, Hongye Yang, Jianfeng Feng, Xiangyang Xue, Qibao Zheng, Xiaoqing Ye, and Xiaolin Zhang. Ssf-dan: Separated semantic feature based domain adaptation network for semantic segmentation. In *Proceedings of the IEEE International Conference on Computer Vision*, pages 982–991, 2019.
- [8] Yaroslav Ganin and Victor Lempitsky. Unsupervised domain adaptation by backpropagation. In *International Conference on Machine Learning*, pages 1180–1189, 2015.
- [9] Yaroslav Ganin, Evgeniya Ustinova, Hana Ajakan, Pascal Germain, Hugo Larochelle, François Laviolette, Mario Marchand, and Victor Lempitsky. Domain-adversarial training of neural networks. *The Journal of Machine Learning Research*, 17(1):2096–2030, 2016.
- [10] Bo Geng, Dacheng Tao, and Chao Xu. Daml: Domain adaptation metric learning. *IEEE Transactions on Image Processing*, 20(10):2980–2989, 2011.
- [11] Ian Goodfellow, Jean Pouget-Abadie, Mehdi Mirza, Bing Xu, David Warde-Farley, Sherjil Ozair, Aaron Courville, and Yoshua Bengio. Generative adversarial nets. In *Advances in neural information processing systems*, pages 2672–2680, 2014.
- [12] Judy Hoffman, Eric Tzeng, Taesung Park, Jun-Yan Zhu, Phillip Isola, Kate Saenko, Alexei Efros, and Trevor Darrell. Cycada: Cycle-consistent adversarial domain adaptation. In *International Conference on Machine Learning*, pages 1994–2003, 2018.
- [13] Judy Hoffman, Dequan Wang, Fisher Yu, and Trevor Darrell. Fcns in the wild: Pixel-level adversarial and constraint-based adaptation. *arXiv preprint arXiv:1612.02649*, 2016.
- [14] Weixiang Hong, Zhenzhen Wang, Ming Yang, and Junsong Yuan. Conditional generative adversarial network for structured domain adaptation. In *Proceedings of the IEEE Conference on Computer Vision and Pattern Recognition*, pages 1335–1344, 2018.
- [15] Lanqing Hu, Meina Kan, Shiguang Shan, and Xilin Chen. Duplex generative adversarial network for unsupervised domain adaptation. In *Proceedings of the IEEE Conference on Computer Vision and Pattern Recognition*, pages 1498–1507, 2018.
- [16] Diederik P Kingma and Jimmy Ba. Adam: A method for stochastic optimization. In *ICLR*, 2015.
- [17] Yunsheng Li, Lu Yuan, and Nuno Vasconcelos. Bidirectional learning for domain adaptation of semantic segmentation. In *Proceedings of the IEEE Conference on Computer Vision and Pattern Recognition*, pages 6936–6945, 2019.
- [18] Jonathan Long, Evan Shelhamer, and Trevor Darrell. Fully convolutional networks for semantic segmentation. In *Proceedings of the IEEE conference on computer vision and pattern recognition*, pages 3431–3440, 2015.
- [19] Mingsheng Long, Yue Cao, Jianmin Wang, and Michael Jordan. Learning transferable features with deep adaptation networks. In *International Conference on Machine Learning*, pages 97–105, 2015.
- [20] Mingsheng Long, Han Zhu, Jianmin Wang, and Michael I Jordan. Unsupervised domain adaptation with residual transfer networks. In *Advances in Neural Information Processing Systems*, pages 136–144, 2016.
- [21] Yawei Luo, Ping Liu, Tao Guan, Junqing Yu, and Yi Yang. Significance-aware information bottleneck for domain adaptive semantic segmentation. In *Proceedings of the IEEE International Conference on Computer Vision*, 2019.
- [22] Yawei Luo, Liang Zheng, Tao Guan, Junqing Yu, and Yi Yang. Taking a closer look at domain shift: Category-level adversaries for semantics consistent domain adaptation. In *Proceedings of the IEEE Conference on Computer Vision and Pattern Recognition*, pages 2507–2516, 2019.
- [23] Andrew L Maas, Awni Y Hannun, and Andrew Y Ng. Rectifier nonlinearities improve neural network acoustic models. In *in ICML Workshop on Deep Learning for Audio, Speech and Language Processing*. Citeseer, 2013.
- [24] Fausto Milletari, Nassir Navab, and Seyed-Ahmad Ahmadi. V-net: Fully convolutional neural networks for volumetric medical image segmentation. In *2016 Fourth International Conference on 3D Vision (3DV)*, pages 565–571. IEEE, 2016.
- [25] Zak Murez, Soheil Kolouri, David Kriegman, Ravi Ramamoorthi, and Kyungnam Kim. Image to image translation for domain adaptation. In *Proceedings of the IEEE Con-*

- ference on Computer Vision and Pattern Recognition, pages 4500–4509, 2018.
- [26] Dong Nie, Yaozong Gao, Li Wang, and Dinggang Shen. Asdnet: Attention based semi-supervised deep networks for medical image segmentation. In *International Conference on Medical Image Computing and Computer-Assisted Intervention*, pages 370–378. Springer, 2018.
  - [27] Yingwei Pan, Ting Yao, Yehao Li, Yu Wang, Chong-Wah Ngo, and Tao Mei. Transferrable prototypical networks for unsupervised domain adaptation. In *Proceedings of the IEEE Conference on Computer Vision and Pattern Recognition*, pages 2239–2247, 2019.
  - [28] Stephan R Richter, Vibhav Vineet, Stefan Roth, and Vladlen Koltun. Playing for data: Ground truth from computer games. In *European Conference on Computer Vision*, pages 102–118. Springer, 2016.
  - [29] German Ros, Laura Sellart, Joanna Materzynska, David Vazquez, and Antonio M Lopez. The synthia dataset: A large collection of synthetic images for semantic segmentation of urban scenes. In *Proceedings of the IEEE conference on computer vision and pattern recognition*, pages 3234–3243, 2016.
  - [30] Kuniaki Saito, Yoshitaka Ushiku, Tatsuya Harada, and Kate Saenko. Adversarial dropout regularization. *arXiv preprint arXiv:1711.01575*, 2017.
  - [31] Kuniaki Saito, Kohei Watanabe, Yoshitaka Ushiku, and Tatsuya Harada. Maximum classifier discrepancy for unsupervised domain adaptation. In *Proceedings of the IEEE Conference on Computer Vision and Pattern Recognition*, pages 3723–3732, 2018.
  - [32] Swami Sankaranarayanan, Yogesh Balaji, Arpit Jain, Ser Nam Lim, and Rama Chellappa. Learning from synthetic data: Addressing domain shift for semantic segmentation. In *Proceedings of the IEEE Conference on Computer Vision and Pattern Recognition*, pages 3752–3761, 2018.
  - [33] Karen Simonyan and Andrew Zisserman. Very deep convolutional networks for large-scale image recognition. In *ICLR*, 2015.
  - [34] Baochen Sun, Jiashi Feng, and Kate Saenko. Return of frustratingly easy domain adaptation. In *Thirtieth AAAI Conference on Artificial Intelligence*, 2016.
  - [35] Yi-Hsuan Tsai, Wei-Chih Hung, Samuel Schuster, Kihyuk Sohn, Ming-Hsuan Yang, and Manmohan Chandraker. Learning to adapt structured output space for semantic segmentation. In *Proceedings of the IEEE Conference on Computer Vision and Pattern Recognition*, pages 7472–7481, 2018.
  - [36] Yi-Hsuan Tsai, Kihyuk Sohn, Samuel Schuster, and Manmohan Chandraker. Domain adaptation for structured output via discriminative representations. In *Proceedings of the IEEE International Conference on Computer Vision*, 2019.
  - [37] Eric Tzeng, Judy Hoffman, Kate Saenko, and Trevor Darrell. Adversarial discriminative domain adaptation. In *Proceedings of the IEEE Conference on Computer Vision and Pattern Recognition*, pages 7167–7176, 2017.
  - [38] Tuan-Hung Vu, Himalaya Jain, Maxime Bucher, Matthieu Cord, and Patrick Pérez. Advent: Adversarial entropy minimization for domain adaptation in semantic segmentation. In *Proceedings of the IEEE Conference on Computer Vision and Pattern Recognition*, pages 2517–2526, 2019.
  - [39] Ken CL Wong, Mehdi Moradi, Hui Tang, and Tanveer Syeda-Mahmood. 3d segmentation with exponential logarithmic loss for highly unbalanced object sizes. In *International Conference on Medical Image Computing and Computer-Assisted Intervention*, pages 612–619. Springer, 2018.
  - [40] Shaoan Xie, Zibin Zheng, Liang Chen, and Chuan Chen. Learning semantic representations for unsupervised domain adaptation. In *International Conference on Machine Learning*, pages 5419–5428, 2018.
  - [41] Ting Yao, Yingwei Pan, Chong-Wah Ngo, Houqiang Li, and Tao Mei. Semi-supervised domain adaptation with subspace learning for visual recognition. In *Proceedings of the IEEE conference on computer vision and pattern recognition*, pages 2142–2150, 2015.
  - [42] Yang Zhang, Philip David, Hassan Foroosh, and Boqing Gong. A curriculum domain adaptation approach to the semantic segmentation of urban scenes. *IEEE transactions on pattern analysis and machine intelligence*, 2019.
  - [43] Yang Zhang, Philip David, and Boqing Gong. Curriculum domain adaptation for semantic segmentation of urban scenes. In *Proceedings of the IEEE International Conference on Computer Vision*, pages 2020–2030, 2017.
  - [44] Yiheng Zhang, Zhaofan Qiu, Ting Yao, Dong Liu, and Tao Mei. Fully convolutional adaptation networks for semantic segmentation. In *Proceedings of the IEEE Conference on Computer Vision and Pattern Recognition*, pages 6810–6818, 2018.
  - [45] Yabin Zhang, Hui Tang, Kui Jia, and Minghui Tan. Domain-symmetric networks for adversarial domain adaptation. In *Proceedings of the IEEE Conference on Computer Vision and Pattern Recognition*, pages 5031–5040, 2019.
  - [46] Hengshuang Zhao, Jianping Shi, Xiaojuan Qi, Xiaogang Wang, and Jiaya Jia. Pyramid scene parsing network. In *Proceedings of the IEEE conference on computer vision and pattern recognition*, pages 2881–2890, 2017.
  - [47] Xinge Zhu, Hui Zhou, Ceyuan Yang, Jianping Shi, and Dahua Lin. Penalizing top performers: Conservative loss for semantic segmentation adaptation. In *Proceedings of the European Conference on Computer Vision (ECCV)*, pages 568–583, 2018.
  - [48] Yang Zou, Zhiding Yu, BVK Vijaya Kumar, and Jinsong Wang. Unsupervised domain adaptation for semantic segmentation via class-balanced self-training. In *Proceedings of the European Conference on Computer Vision (ECCV)*, pages 289–305, 2018.